Journal of Sound and Vibration (2001) **244**(5), 761–778
doi:10.1006/jsvi.2000.3536, available online at http://www.idealibrary.com on IDEAL®

COMPARISON OF STRUCTURAL–ACOUSTIC CONTROL DESIGNS ON AN ACTIVE COMPOSITE PANEL

B. Bingham, M. J. Atalla and N. W. Hagood

Department of Aeronautics and Astronautics, Massachusetts Institute of Technology, Cambridge, MA 02139, *U.S.A. E-mail: bbing@mit.edu*

(*Received* 31 *August* 1999, *and in final form* 14 *November* 2000)

This work presents a comparison of three technologies for structural–acoustic control that, while prevalent in the literature, had not been compared on a single structure. The comparison is generalizable because the techniques are implemented on a panel structure representative of a more complex structure (e.g., an aircraft fuselage, a submarine vehicle hull, a satellite payload shroud, etc.). The test-bed used for this comparison is a carbon-fiber composite panel manufactured with embedded active fiber composite actuators. Since such integrated structures constitute a continued avenue of research, the manufacturing and performance of this structure is illustrated. The design of the test-bed is guided by an effort to achieve a dynamic response similar to a single panel in a typical aircraft or rotorcraft fuselage.

Existing active control architectures for broadband acoustic radiation reduction are compared both analytically and experimentally on a representative structure to quantify the capabilities and limitations of the existing control methodologies. Specifically, three broad categories of control are compared: classical feedback (rate feedback), optimal feedback (linear quadratic Gaussian), and adaptive feedforward control (x-filtered least mean square). The control architectures implemented during this study are all single-input/single-output in order to allow a fair comparison of the issues involved in the design, as well as the use and performance of each approach. Both the vibration and the acoustic performance are recorded for each experiment under equivalent conditions to allow a generalizable comparison. Experimental results lead to conclusions pertaining to the application of active structural-based control to improve the acoustic performance of more complex structures.

1. INTRODUCTION

Actively reducing noise levels resulting from mechanical vibrations can increase reliability and user satisfaction while reducing costs and expanding capabilities of a variety of high-performance structures. The goals of this work are to present a fundamental analysis of the structural–acoustic system and demonstrate how active materials can be integrated into the structural design to reduce the radiated sound power. A representative structural element is considered and various control methods are implemented in simulation and experiment to quantify the limitations and capabilities of each approach. The analysis presented is meant to be general; the goal is not to design an optimally performing single panel, but to keep the elements of the problem generic, allowing the application of the resulting insight to more complex applications.

An overview of the historical development of the active acoustic control is presented in reference [1]. First attempts at noise control utilized secondary acoustic sources and sensors to cancel the primary disturbance source. It has been shown that multiple sources

0022-460X/01/300761 + 18 $35.00/0

can be utilized to produce both local and global quieting [2, 3]. This approach has been termed active noise control (ANC). This is contrasted with the more recent investigations in the field of active structural–acoustic control (ASAC) or active vibration and acoustic control (AVAC), utilizing structural-based sensors and actuators in order to reduce the acoustically radiating structural vibrations. ASAC eliminates the need for loudspeaker acoustic actuators and microphone error sensors within the acoustic medium which can add unsatisfactory weight and costs to the overall design. With the advances in adaptive structures, recent work has focused on integrating sensing and actuation within the structure. Current research has focused on two canonical structures, flat panels and smooth cylinders, which can be analyzed relatively simply to investigate the physics of the structural–acoustic coupling. Work on simple plate structures began with the application of feedforward techniques to reduce a single frequency (tonal), known disturbance with point force [4] or acoustic control inputs [5]. More recently, system designs that utilize surface sensors to estimate the acoustic radiation, and surface-mounted piezoelectric elements as control inputs have been implemented [6]. Each of the aforementioned investigations concentrates on variants of the least mean squares (LMS) feedforward control algorithm. Causality and convergence can limit the bandwidth and applicability of such compensation techniques [7], but for applications where a known source dominates the disturbance energy, this tonal or narrowband approach achieves significant performance. An example compares the tonal control system using both structural (PVDF) and acoustic (microphone) sensing [8]. For broadband structural actuation, the LMS algorithm must be extended using an experimental model of the structural transfer function relating the input and output [9]. The resulting x-filtered LMS (xLMS) algorithm has been shown to yield broadband acoustic radiation reduction on a lightly damped structure.

As technical challenges of ASAC are met, an increasing number of applications become possible. To apply the basic achievements in materials, maufacturing, and control theory to complex structures and to achieve the potential acoustic performance, an understanding of the trade-off involved in integrating these advances must be realized. With the goal of implementing ASAC on more complex structures [10], this paper presents a set of analytic and experimental results answering fundamental questions revelant to designing active structural–acoustic controllers.

The goal of this work is to bring the scientific advances outlined previously closer to applications currently under investigation. The organization of this work is meant to highlight this purpose. A single flat panel is used as a test-bed for implementing a variety of control techniques. The flat panel is a representative structure—it is dynamically complex enough to gain a full appreciation of challenges of structural–acoustic control, while being simple enough to allow analytic modeling for a level of understanding of the dynamics that is not currently achievable in more complex applications.

This paper is organized in parallel with the actual work that was completed. First the structural–acoustic model is presented. This model is used (in conjunction with an experimentally identified structural model) for controlling the acoustic radiation from structural sensors and is included in the development of a class of compensators. Next the experimental test-bed, a composite panel with embedded active fiber composite (AFC) is presented in detail because of the issues regarding the manufacture of integrated composite structures that are still under investigation. The details of the structural–acoustic control designs are included to illustrate the engineering judgement that is present in the design of any compensator that is to be implemented in hardware. In particular, the first experimental implementation of the acoustic radiation filters proposed by Baumann *et al.* [14] is reported together with experimentally measured performances of every design

implemented. Finally, the results are summarized and expressed through a comparison of the techniques implemented. Further details are available in a detailed report [11].

2. ANALYTICAL STRUCTURAL–ACOUSTIC MODEL FOR CONTROL

A detailed model of the structural–acoustic system is necessary for both control design and performance simulations. For this investigation the structural and acoustic models are considered independently. A Rayleigh–Ritz modeling formulation [12] and classical laminated plate theory [13] were used, but will not be presented for brevity. Due to the characteristics of the chosen test-bed, a high fidelity structural model can be developed and used to understand the dynamic behavior and structural–acoustic coupling of the system. However, as is often the case when implementing modern control designs, it is necessary to use an experimentally identified model to build the actual compensator.

While many designs rely on a reduction in vibration levels to achieve a reduction in acoustic radiation, a representation of how the vibration is transformed into acoustic energy allows the design of compensators that can directly target the acoustic radiation (e.g., incorporating such a model into the cost function expression for a linear quadratic Gaussian (LQG) compensator). Towards this end a radiation model is developed to understand the structural–acoustic coupling for a flat panel. Two simplifying assumptions are made in the model development—the surrounding medium is considered as a light fluid and the radiated acoustic power measurement is assumed to be made in the far field. By assuming the former, the structure is considered to vibrate in vacuo and the induced acoustic pressures and velocities are obtained based on the representation of the structural motion. For acoustic applications in air, this assumption is normally valid. The farfield measurement assumption allows the use of the characteristic impedance of the medium, therefore allowing the analytic development of the expression for the radiated power.

2.1. ACOUSTIC RADIATION FROM FLAT PANELS

To predict the closed-loop acoustic performance it is necessary to model the acoustic radiation from the vibrating structure. For simple structures such as baffled panels and infinite cylinders, the radiation problem is greatly simplified due to the geometry. The Rayleigh integral completely describes the acoustic pressure field resulting from a planar vibrating source in an infinite baffle as a function of the vibration profile. This is used, along with the farfield assumption, to express the radiated power as a function of the modal velocities of the structure—states of the previously mentioned structural model. This approach, originally proposed by Baumann *et al.* [14], is experimentally verified here for the first time (to the best of the authors' knowledge). Its derivation is presented here to emphasize its applicability and restrictions to real-time digital structural-acoustic control.

From the linear acoustic wave equation, the general acoustic radiation problem can be formulated as a single integral equation, the Kirchoff–Helmholtz equation. For flat sources, the equation can be further simplified to a succinct expression for the pressure in the medium as a function of the surface vibration—the Rayleigh integral.

$$p(\mathbf{r}) = \frac{i\omega\rho}{2\pi} \iint_S \frac{v_n(\mathbf{r}_s) e^{-ik|\mathbf{r}-\mathbf{r}_s|}}{|\mathbf{r}-\mathbf{r}_s|} dS. \tag{1}$$

The Rayleigh integral (1) is a general expression of the total pressure field in the medium (i.e., both near and far field) at an observation point ($\mathbf{r}$), as a surface integral of the normal

surface velocity (v_n) which is a function of the position on the planar structure ($\mathbf{r}_s$). The pressure is also a function of the density of the surrounding medium (ρ), the acoustic frequency (ω), and the acoustic wave number (k).

The total radiated acoustic power is an attractive performance metric for acoustic control. The expression for the radiated pressure can be used to evaluate the total power under the assumption that the impedance at the outer boundary is equivalent to the characteristic impedance of the fluid, ρc, where c is the propagation speed of sound in the medium. This simplification assumes that the power is measured in the far field where the waves radiate spherically. To evaluate this integral analytically for the case of a simply supported plate, the far field assumption is enforced on the evolution of the scalar observation distance ($\bar{R} = |\mathbf{r} - \mathbf{r}_s|$). The distance, $\bar{R}$, is present in two terms in the Rayleigh integral, and two different approximations are made to simplify the expression. First, a geometric restriction is introduced as the observation distance is assumed to be much greater than the characteristic dimension of the structure, implying the approximation $\bar{R} \approx r$ in the denominator of equation (1). However, the exponential term must be treated differently since the phase relationship is critical to the validity of the integration. Here, the observation distance is linearized about the point $r = \mathbf{r}$, $\varphi = 0$, $\theta = 0$, leading to the approximation

$$\begin{aligned}\bar{R} &= \sqrt{(r\sin(\theta)\cos(\phi) - x)^2 + (r\sin(\theta)\sin(\phi) - y)^2 + (r\cos(\theta))^2} \\ &\approx r - x\sin(\theta)\cos(\phi) - y\sin(\theta)\sin(\phi). \end{aligned} \tag{2}$$

This allows for the dependence on the radius to be removed from the integrand, but it limits the analysis to solutions for the far field pressure at low frequencies. To satisfy this assumption the following frequency restrictions,

$$ka \ll 1 \quad \text{and} \quad \lambda \gg 2\pi a, \tag{3}$$

must be met, where a is the characteristic dimension of the panel and k is the acoustic wave number. The composite panel used as test-bed in this work has a characteristic dimension of 0·3 m. Using the properties of air, $c \approx 343$ m/s, the spatial restriction is satisfied for $r > 3a \approx 1$ m, and the frequency condition requires that $\omega \ll c/a = 1143$ Hz (or $\lambda \gg 2\pi a = 3\pi/5 \approx 1{\cdot}9$ m).

Noting these restrictions and substituting the eigenfunctions for an isotropic, homogeneous plate with simply supported boundary conditions, the farfield Rayleigh integral expresses the pressure as a sum of panel mode contributions which can be integrated analytically [15]. Using the characteristic impedance and integrating over a hemisphere, the radiated power is expressed as a generalized inner product of the structural modal velocity vectors, $\dot{\eta}$, which are the states of the structural state-space model:

$$\Pi(\omega) = \dot{\eta}^{\mathrm{T}} M(\omega)\dot{\eta}. \tag{4}$$

The radiation matrix, $M(\omega)$, expresses the relationship between the modal velocities and the radiated power as an integral equation which can be evaluated numerically:

$$M(\omega) = \frac{k^2(\rho c)(L_x L_y)^2}{8\pi^6} \int_0^{2\pi}\int_0^{\pi/2} [mm^H]\sin(\theta)\,\mathrm{d}\theta\,\mathrm{d}\phi,$$

$$m = \left(\frac{1}{(pq)}\right)\left[\frac{(-1)^p\,\mathrm{e}^{-i\alpha} - 1}{(\alpha/p\pi)^2 - 1}\right]\left[\frac{(-1)^q\,\mathrm{e}^{-i\beta} - 1}{(\beta/p\pi)^2 - 1}\right], \quad \begin{aligned}\alpha &= kL_x\sin(\theta)\cos(\phi), \\ \beta &= kL_y\sin(\theta)\sin(\phi).\end{aligned} \tag{5}$$

The modal velocities are indexed by the integer number of half wavelengths in the x and y co-ordinate directions, p and q respectively, in equation (5). The examination of the radiation matrix lends a degree of insight into how the individual mode shapes radiate acoustically. The radiation efficiency, σ, of a particular mode shape is defined as the power radiated by a particular velocity profile normalized by the power radiated by a rigid piston radiating with the same average velocity:

$$\sigma_i = \frac{\Pi_{mode\ shape}}{\Pi_{rigid\ piston}} = \frac{8}{\rho c L_x L_y} M_{(i,\,i)}(\omega). \tag{6}$$

Figure 1 shows the radiation efficiency of the diagonal, or self-radiating terms, of the radiation matrix for nine simply supported panel modes. The geometry used in this simulation corresponds to the experimental set-up. The abscissa of the plot is normalized by the individual structural wave numbers ($k_p \equiv \sqrt{((p\pi)/L_x)^2 + ((q\pi)/L_y)^2}$) to emphasize the critical frequencies, where the structural and acoustic wave numbers are equivalent. The figure illustrates the high structural–acoustic coupling of the odd modes, or volumetric modes, in comparison to the even modes of the simply supported panel. The radiation matrix also captures the radiation coupling between modes, represented by the off-diagonal terms in the radiation matrix, which are not shown in Figure (1). It is important to note that these terms cannot be neglected when representing the total radiated acoustic power. To capture all the radiating power at a given frequency, the contributions from each of the constituent modes must be included, and neglecting the coupling (off-diagonal) terms greatly underestimates the radiated power.

Numerically solving equation (5) yields a set of harmonic solutions for the structural mode shapes at discrete frequency points. This numerical data can be approximated using Laplace-domain multiple-input, multiple-output transfer functions $M(s)$, known as

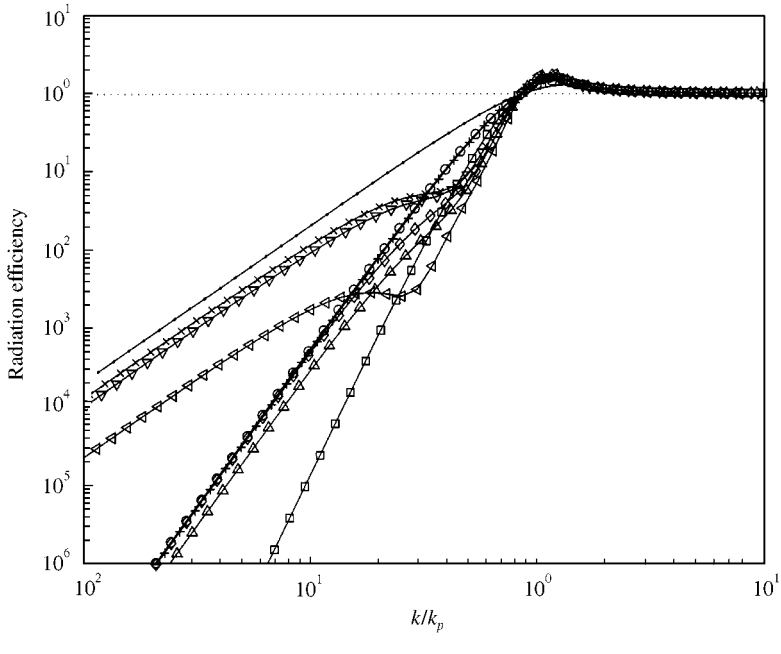

Figure 1. Radiation efficiency of simply supported panel mode. The structural modes shown above are: ●, (1, 1) ○, (1, 2); ×, (1,3); +, (2, 1); □, (2, 2); ◇, (2, 3); ∇, (3, 1); △, (3, 2); ◁, (3, 3).

radiation functions. Since one of the goals of this research is to experimentally implement, validate, and quantify the performance of acoustic radiation filters, it is very important to incorporate this radiation model into the optimal control formulation (see section 4.2). In order to accomplish this, it is necessary to spectrally factorize the system into a stable, causal radiation filter, $G(s)$:

$$M(s) = G^{\mathrm{T}}(-s)G(s). \tag{7}$$

Two main methods have been suggested in the literature for the spectral factorization. A direct state-space approach, presented in reference [16], while theoretically straightforward is numerically difficult to implement. A method specially developed for power spectral factorizations, presented in reference [17], is algorithmic and relies on subspace techniques to derive a factorization. It was found during this research that the best method is to perform a standard eigenvalue decomposition, since the positive real radiation matrices at each harmonic frequency (ω_i) are guaranteed to have positive, real eigenvalues. Each matrix is factored individually by performing an eigenvalue decomposition:

$$M(\omega_i) = V \Lambda V^{\mathrm{T}} = G^{\mathrm{T}}(\omega_i)G(\omega_i), \quad G(\omega_i) = \sqrt{\Lambda} V^{\mathrm{T}}. \tag{8}$$

In order to decompose the radiation matrix into radiation modes at each acoustic frequency, the eigenvectors need to be sorted and normalized so that the diagonals of the eigenvector matrix (V) are positive and maximum for each eigenvector. If this step is not included, the difficulties recounted in reference [18] are encountered, i.e., an *a priori* parameterization is difficult to discern. By consistently ordering the eigenvectors in this manner, the cross-coupling between modes (resulting from the off-diagonal terms of the radiation matrix) is reduced, thus reducing the order of the realization required to capture the behavior. Since the factorization is accomplished prior to the model generation, a state-space system with left-half plane poles and zeros can be fitted to the numeric results to realize the spectrally factored system, $G(s)$.

A characteristic of the suggested factorization and Laplace-domain model is that it can be expressed in the time domain as a state-space system for control design, allowing for real-time digital implementation of this method. This formulation allows for a very simple coupling between the structural and acoustic models. Since the states of the structural model (either an analytical or an experimental model) contain the modal velocities, the radiation matrix can be directly appended to the structural model yielding a state-space model of the structural–acoustic system that relates the system inputs and disturbances to the sensor outputs and the far field radiated acoustic power. The resulting structural–acoustic state-space model is exactly what is needed to both design modern compensators and simulate the performance of various control techniques.

3. EXPERIMENTAL TEST-BED: COMPOSITE PANEL WITH EMBEDDED ACTUATION AND SENSING

This section describes the test-bed panel and explains the canonical experimental procedure. The structure chosen is novel and important for developing technologies, such as multi-functional composites. The composite panel used in this work contains embedded active fiber composite actuators and strain gauge sensors. Embedded actuation of composite structures continues to be an avenue of research and application [19]. The dimensions of the panel, $10{\cdot}3'' \times 12''$, are chosen to have a dynamic response similar to a single panel of a typical commercial aircraft or rotorcraft fuselage panel [10]. Since the

panel was taken to be representative of more complex structures, the results obtained here have led to developments in similar problems [20–23].

The basis for the composite laminate is a quasi-isotropic lay-up typical in applications which benefit from the increased stiffness and strength to weight ratio of composite structures. A quasi-isotropic laminate has equivalent extensional stiffness in the two in-plane directions and no bend–twist coupling. For this panel an eight-ply symmetric lay-up, denoted by $[0/\pm 45/90]_s$, of graphite/epoxy (AS4/3501-6, 32% resin from Hexcell Corp.) is used as the nominal passive lay-up. To accommodate the embedded sensors and actuators and provide a measure of electrical isolation, three E-glass host plies (450-1/2 glass fabric with F155 resin system from Hexcel Corp.) were incorporated into the lay-up for each active ply. A ply the full size of the panel was included both above and below the two active layers while material was removed from the middle layer of E-glass in order to incorporate the active fiber composites ($2'' \times 3''$ AFC's from Mide Technology Corp. [24]) with minimal thickness discontinuities. The full lay-up is illustrated by the typical cross-section shown in Figure 2.

Three critical issues need to be addressed when incorporating structural sensors and actuators into laminate structures: isolation, shielding, and connections. Active fiber composites (AFC's) require very large driving potentials, demanding that the power leads be well insulated from the surrounding conductive graphite plies. Kapton encapsulated flexible circuits (All Flex, Inc.) were placed between the outermost insulating E-glass ply and the host E-glass ply (see Figure 2). Strain guages (0/90° T-Rosettes from Measurements Group—CEA-06-062UT-120) were also embedded within the panel with the intent of using the strain measurements as control sensors. Strain guage sensors are very sensitive to electro-magnetic field disturbances, such as the high electrical fields from the AFCs, and require proper shielding in order to accurately measure strain. Robust connections to the actuation and sensing elements were designed to survive the harsh environment of a composite cure (e.g. 350°F and 85 psi).

Figure 3 shows the positioning of the embedded elements in the composite test panel. AFC elements were embedded in the structure to provide uniaxial actuation of the structural modes of the panel and the coupled acoustic transmission. In addition to their uni-directional authority, their compliance and electrical isolation are distinct advantages for embedding the elements within composite structures. The interdigitated electrode pattern is shown on the individual AFC elements and the fiber direction is perpendicular to the electrode lines. Each of the actuator pairs is placed symmetrically about the neutral axis at the indicated locations, and electrically connected 180° out-of-phase to produce

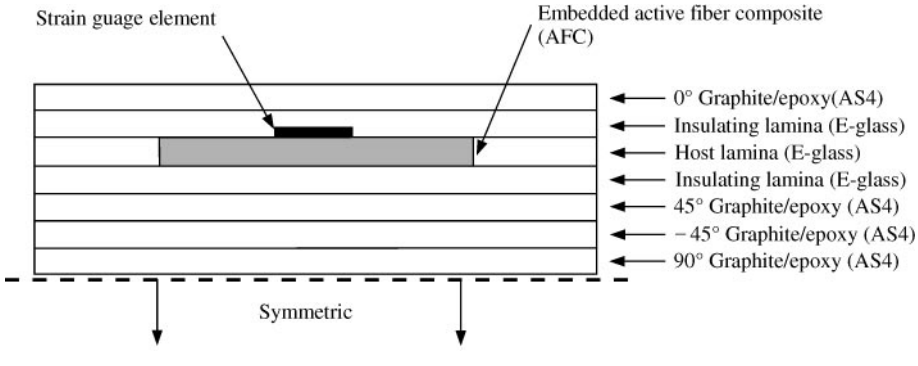

Figure 2. Lay-up of experimental composite panel (typical dimensions: AS4 Graphite, 5·28 mil; E-glass, 4·75 mil; AFC, 8·1 mil; Strain Guage, 11·7 mil).

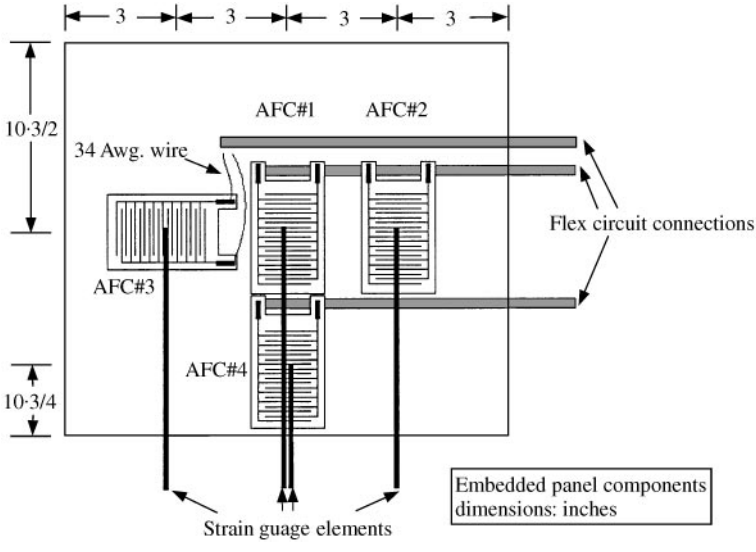

Figure 3. Layout of experimental composite panel.

a bending moment. The embedded strain sensors successfully measured the strain at the locations under piezoelectric actuation, but were not used in the closed-loop experiments because of excessive sensor noise.

The composite panel was mounted in one wall of an anechoic chamber (Industrial Acoustics Co.) with low frequency cut-off measured to be less than 120 Hz. To approximate the simply supported boundary conditions, thin shim steel flexures (0.01″) were used to attach the panel to the rigid frame. A 1/4″ fold is made in the shim in order to bond it to the composite panel using structural epoxy (EPON 828 resin with EPI-CURE 3223 curing agent, Shell Inc.). A baffle was constructed in the plane of the panel, extending to the edges of the anechoice chamber opening. A single panel of 1/4″ sheet rock was used to interface with the composite test-bed and two additional sheet rock panels were included behind the test set-up to further reduce the transmission through the baffle (see Figure 4). The baffle serves two purposes; it blocks the transmission of sound from the external environment, while separating the influence of the two radiating sides of the panel. The experimental set-up is shown in Figure 4 with the microphone traverse used to measure the acoustic pressure inside the chamber.

4. STRUCTURAL–ACOUSTIC CONTROL: DESIGN, IMPLEMENTATION, AND PERFORMANCE RESULTS

Structural–acoustic control aims at modifying the surrounding acoustic field by controlling structural motion. The most widely used vibration control methods can be classified as classical feedback control, optimal feedback control, adaptive feedforward control, and feedforward or feedback neuro-fuzzy control. When applied to structural–acoustic control problems, adaptive feedward controllers have drawn most of the attention. However, when a reference signal is not available it becomes necessary to use some form of feedback control based on structural information. In this paper four control methods are explored both analytically and experimentally to determine their relative

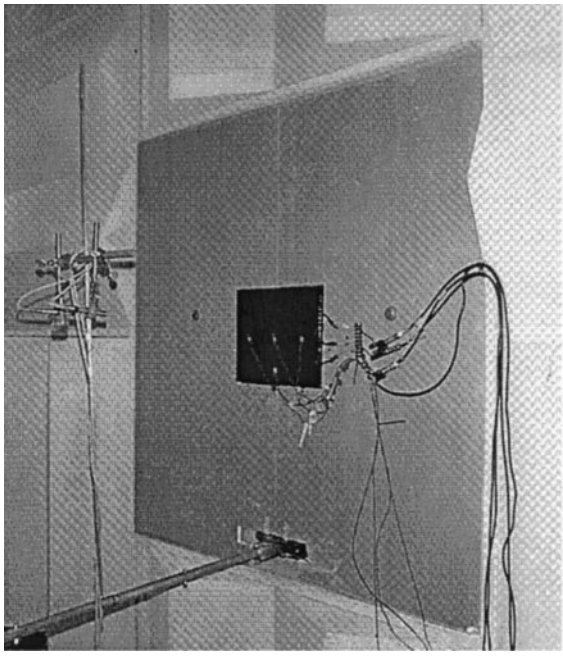

Figure 4. Baffled composite panel in anechoic chamber with microphone traverse.

merits for structural–acoustic control applications. Specifically, classical feedback, optimal feedback, using frequency weighting functions and radiation filters, and adaptive feedforward methods are investigated in what follows and implemented on the active composite panel test-bed described in the previous section.

This work presents a comparison of four methods of structural–acoustic control that, while prevalent in the literature, had not been compared on a single structure. The comparison can be generalized since the structure is a representative structure, used in many complex structures such as aircraft fuselage, satellite payload shroud, etc. The control architectures implemented in this research are all single-input/single-output in order to allow a fair comparison of the issues involved in the design, use and performance of each approach. The implementation of multi-input/multi-output (MIMO) controllers would introduce other variables to the problem, such as engineering judgment in fitting a model from the experimental data (LQG), multiple control to error signal paths (xLMS), and lack of good classic control design tools for MIMO systems, making a fair comparison difficult to achieve.

Single-input/single-output (SISO) controllers were designed and implemented using each of the three architectures mentioned above. The results that follow are based on a canonical, structural–acoustic, closed-loop experiment using a single AFC pair ($\#1$) as the control input, a surface mounted accelerometer (Endevco 2222C/2721B conditioner) placed on top of AFC pair $\#1$ as the feedback sensor, and a single AFC pair ($\#2$) as the disturbance source. A dSPACE real-time control system is used to implement the digital compensator designs at a sampling rate of $1{\cdot}5 \times 10^{-4}$ s. The system consists of a dedicated DSP processor (TMS320C40-60 MHz on a DS1003-256 board) connected to input/output hardware (DS2003 A/D converter and DS2103 D/A converter) via a high-speed bus. Anti-aliasing filters were used at both the input and the output of the digital compensator using digitally

programmable analog Bessel filters (Frequency Devices 824L8L5). The scaled control and disturbance signals are amplified (Yorkville AudioPro 3400 amplifiers with custom 25 : 1 voltage step-up transformers) in order to generate the high-voltage signals necessary for AFC actuation. A spectrum analyzer (DSPTechnology, Inc., SigLab 20–42) was used to acquire the frequency response functions used to characterize the open- and closed-loop systems.

The closed-loop performance was measured by estimating the root mean square reduction from open- to closed-loop frequency response in decibels (dB). The vibration performance can be measured directly from the frequency response function by numerically integrating the open- and closed-loop transfer functions. The radiated acoustic power was estimated by measuring the acoustic frequency response at discrete locations in a mid-plane arc about the panel in order to measure the acoustic performance. The broadband dB reduction metric is used consistently in order to compare the results to follow.

4.1. CLASSICAL CONTROL (RATE FEEDBACK)

Simplicity of implementation and robustness to modelling errors make classical techniques very attractive. For complex applications where no accurate model is available classical techniques may be the only tractable solution. Classical techniques attempt to actively damp the vibration, indirectly reducing the acoustic radiation. The effectiveness of this indirect approach is highly dependent on the placement of the sensors and actuators.

A convenient relationship can be exploited in structural control when rate feedback controls is utilized on collocated and dual sensor/actuator pairs as described at length in reference [25]. This architecture results in an actuator to sensor transfer function that is positive real for all frequencies, that is, the phase of the loop transfer function is bounded by $\pm 90^\circ$ and the poles and zeros alternate with increasing frequency. This particular structure allows for a general robustness guarantee often referred to as hyperstability. This type of design, however, is subject to practical limitations. First the actuator and sensor dynamics, typically important at higher frequencies, make it necessary to have finite bandwidth in the control loop, i.e., the loop becomes no longer truly hyperstable. To limit the bandwidth, additional dynamics are introduced into the experimental control loop to reduce the high frequency gain in the transfer function from actuator to sensor, i.e., increase the rate of roll-off. While the sensor/actuator pair used here (AFC-accelerometer) is not truly a collocated, dual pair, the transfer function is positive real for a bandwidth sufficiently high to utilize the robustness of the collocated dual architecture, enabling a simple control design. The design is performed by inspecting the control input to sensor output open-loop dynamics, therefore not requiring an analytical model.

The compensator designed contains a single pole that stabilizes the system by reducing the high frequency gain, but causes additional phase lag, reducing the phase margin. By placing the pole at 600 Hz, the low-frequency modes of the panel are controlled and the compensator is gain stabilized at higher frequencies where the digitial implementation would be unstable due to the quantization effects and unmodelled dynamics. The scalar gain parameter was iteratively adjusted to maximize the acoustic performance. Both the vibration and the acoustic performance of the system are illustrated in Figure 5. The compensator reduces the vibration level as measured by the central accelerometer by 0·83 dB, and as a result the far field acoustic radiation was reduced by 1·96 dB. From the plots comparing the open- and closed-loop frequency responses, it is evident that the reduction is achieved by adding damping to the resonant modes of the structure.

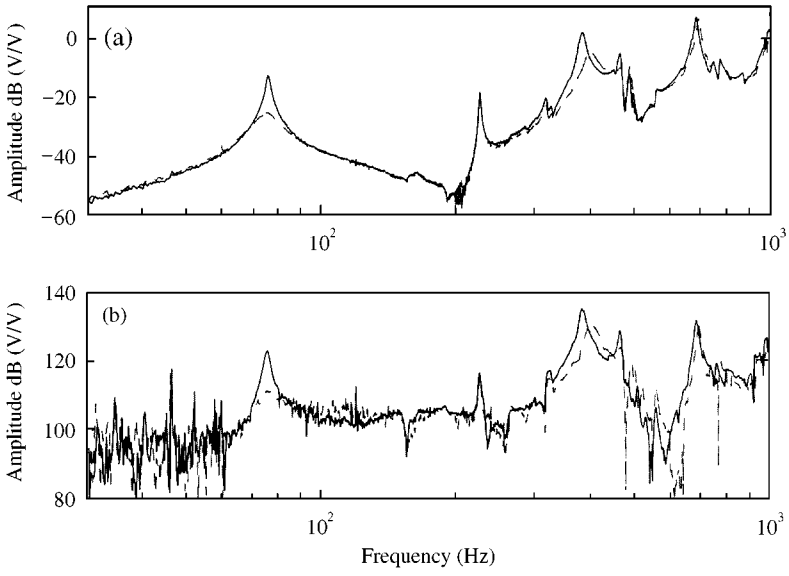

Figure 5. Performance of rate feedback control (——, open loop; – – – –, closed loop). (a) Vibration performance 0·83 dB, (b) acoustic performance 1·96 dB.

4.2. OPTIMAL CONTROL (FW-LQG AND RF-LQG)

Optimal control theory has been extensively developed for a variety of applications [26, 27]. The formulation presented here follows the notational conventions presented by Lublin [27], making inclusion of the radiation filter model quite simple. This section presents just the essential background information necessary to present the experimental results and emphasizes the application of model-based optimal control, particularly linear quadratic Gaussian (LQG) design methods, to the problem of structural–acoustic control.

To illustrate the two LQG designs implemented, the cost functions for each of the two compensator designs are shown below. The LQG cost function embodies the optimal control design which seeks to minimize both the performance cost, a function of the states of the structural system ($x(t)$), and the control cost, a function of the control signal ($u(t)$). The first cost formulation, equation (9), simply minimizes the vibration as sensed by the structural sensor, hence it attempts to reduce the acoustic radiation indirectly by mitigating the vibration of the structure. This type of compensator will be termed a frequency-weighted LQG design (FW-LQG). The matrix C_z is the measurements matrix and the constant ρ represents the control cost relative to the states of the system:

$$J_{structural} = \lim_{\tau \to \infty} \frac{1}{\tau} \int_{\tau} [x^{\mathrm{T}}(t) C_z^{\mathrm{T}} C_x x(t) + \rho u^{\mathrm{T}}(t) u(t)] \, \mathrm{d}t. \tag{9}$$

The second formulation, equation (10), utilizes the acoustic model to directly minimize the radiated acoustic power ($\Pi(t)$). The radiation filter obtained in equation (8) from section 2.1 is converted from the frequency domain to a state-space model, (G_t), allowing for a simple expression of the acoustic optimal cost function in terms of the structural states of the system. It should be noted that the radiation filter is time invariant, but the notation G_t is used to distinguish the time-domain implementation from the frequency-domain radiation filter resulting from the factorization of the radiation matrix in equation (8). This

formulation will be termed the radiation filter LQG design (RF-LQG):

$$J_{acoustic} = \lim_{\tau \to \infty} \frac{1}{\tau} \int_{\tau} [\Pi(t) + \rho u^{\mathrm{T}}(t) u(t)] \, \mathrm{d}t$$

$$= \lim_{\tau \to \infty} \frac{1}{\tau} \int_{\tau} [x^{\mathrm{T}}(t) G_t^{\mathrm{T}} G_t x(t) + \rho u^{\mathrm{T}}(t) u(t)] \, \mathrm{d}t. \tag{10}$$

Based on the two LQG optimal control cost functions presented above, two model-based compensators were implemented on the composite panel. In order to design this type of control system, a very accurate model of the structural system was required, making it necessary to synthesize a state-space structural model from experimental data. The frequency domain observability range space extraction (FORSE) [28] method was used to fit a parametric model to the experimental frequency response data. A 22 state 2 input (control and disturbance), single output (sensor) model synthesized from frequency response data up through 2 kHz was used in designing the LQG compensators.

Frequency-weighting techniques were used to design a FW-LQG controller to minimize the vibration response at the structural sensor location. Two weighting functions, one on the state cost and one on the control cost, were used to tailor the performance of the system. The fourth order state-weighting filter consists of a second order bandpass filter with a center frequency at 75 Hz and damping ratio of 0·3 to concentrate the control effort near the first resonant mode. Additionally, a complex pole pair at 750 Hz with a damping ratio of 0·5 was used to limit the bandwidth of the compensator. A fourth order control-weighting function was used to ensure the limited bandwidth of the compensator, preventing the compensator from destabilizing at higher frequencies. Figure 6 shows the vibration and radiation performance for the frequency-weighted LQG (FW-LQG) compensator designed to minimize the accelerometer signal. The 4·56 dB in vibration reduction and 5·93 dB in acoustic reduction are achieved by attenuating the response at the resonant frequencies.

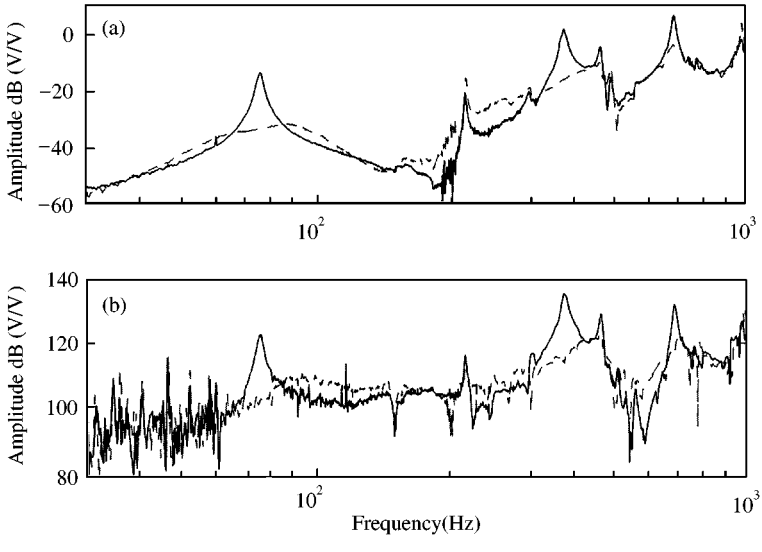

Figure 6. Performance of LQG design using structurally based cost function (FW-LQG) (——, open loop; – – – –, closed loop). (a) Vibration performance 4·56 dB, (b) acoustic performance 5·93 dB.

This is consistent with the LQG design methodology which, due to the cost function expression, attempts to minimize the root mean square (H_2 norm) response of the system.

A second LQG compensator was designed using the radiation filter model (RF-LQG). A 24 state realization of the radiation filter, $G(s)$, was achieved using the balance reduction technique [26] and found to be within the capabilities of the digital control computer. The final compensator is implemented as a digital 15 state, state-space model with a sampling period of $1{\cdot}5 \times 10^{-4}$ s. The non-linear process of converting the optimal designs to a digital implementation was performed iteratively in order to find a realization with stability margins similar to the full-state, continuous time compensator. Figure 7 shows the performance of the RF-LQG design which uses the frequency weighting providing by the radiation filter acoustic model. The closed-loop response is very similar to that observed in the FW-LQG design of Figure 6 as the performance is achieved by reducing the resonant response. The broadband reduction in the response is of 4·27 dB for the acceleration response and 4·13 dB for the radiated acoustic response.

In this comparison, the LQG controller designed using the radiation model achieved slightly less performance than the controller designed based solely on the vibration sensor, illustrating a very important dichotomy between control and system design. Since the vibration sensor is placed at the center of the panel, the measured acceleration is dominated by the odd-odd or volumetric modes of the structure. This allows control of the vibration as measured at this location to achieve acoustic performance, but this result is highly dependent on the sensor and actuator placement. In contrast, the radiation filter serves to estimate the radiated power based on a single structural measurement. Placing the sensor on another spatial location would have little effect on the resulting acoustic performance as long as the radiating modes of the structure are observable. Another factor contributing to these results is the iterative nature of the FW-LQG compensator design. The frequency-weighted LQG compensator was designed by shaping the frequency response to achieve the best performance while remaining stable. This allows a considerable amount of freedom and demands a fair amount of iteration. Implementing the radiation filter is done

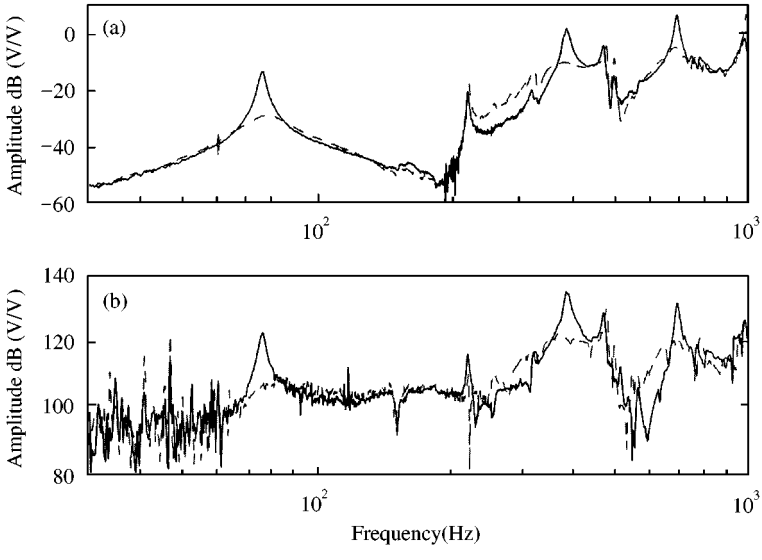

Figure 7. Performance of LQG compensator designed using the acoustic cost formulation (RF-LQG) (——, open loop; – – – –, closed loop). (a) Vibration performance 4·27 dB, (b) acoustic performance 4·13 B.

with less iteration as the basic loop shaping is done using the model. Applying the radiation filter in an engineering system would demand an approach that was a hybrid of the two using both the analytical tool and intuition of the designer.

4.3. ADAPTIVE FEEDFORWARD CONTROL (*x*LMS)

As an estimation technique, the adaptive LMS algorithm is used in a variety of applications [29]. LMS feedforward acoustic control was originally presented as a method for noise cancellation using secondary acoustic sources [30]. It was shown that considerable noise cancellation can be achieved when the primary and secondary sources are separated by less than one half the wavelength of the acoustic disturbance. The control design is simple to implement; the finite impulse response (FIR) estimator is adaptively updated using only the measured error and disturbance signals, but requiring explicit knowledge of the disturbance source signal. As research in acoustic control moved from using secondary sources in the medium to utilizing structural sensing and actuation, the LMS algorithm has been extended for use with structural sensors [31]. The *x*-filtered version of the LMS controller (*x*LMS) implements an infinite impulse response (IIR) filter model of the control to error signal path to modify the disturbance signal.

Three key components of the *x*LMS algorithm highlight the architectural comparison with feedback compensation. First, the disturbance, or a signal coherent with the disturbance, must be known *a priori* and fed forward to the adaptation algorithm in order to perform the adaptation of the finite impulse response (FIR) filter coefficients. Second, similar to the LQG control designs, the compensator must contain a model of the control input to error sensor output relationship. The prefiltering of the disturbance signal using this linear system is the key extension in the *x*-filtered version of the algorithm. The time invariant infinite impulse response (IIR) prefilter allows an adaptive FIR filter to estimate the behavior of a resonant structural plant with a minimum number of filter coefficients [9]. This is necessary to implement the adaptive filter with few enough states to be computationally tractable. Third, the *x*LMS compensator attempts to minimize the square value of the sensor error. This is analogous to the version of the LQG compensator design which targets the sensor error (equation (9)), in that the acoustic control is implicit in the vibration reduction. It becomes necessary to implement an acoustic sensor, or to estimate the acoustic radiated power based on structural measurements, to directly include the acoustic performance in the compensator.

An adaptive feedforward (*x*LMS) compensator was implemented in a similar experiment in order to directly compare the performance of the feedback and feedforward designs. The implementation of the *x*LMS algorithm uses the normalized LMS version of the adaptive finite impulse response estimator to minimize the sensor error signal [29]. The disturbance signal, a random noise input, is fed directly to the compensator in order to perform the adaptation. Similar to the frequency-weighted LQG design, this compensator mitigates the acoustic radiation indirectly by reducing the vibration levels in the structure at the error sensor. Preliminary experiments illustrated, as expected, the enhanced performance with increased filter order. The model of the control path is implemented using the same FORSE state-space model used in the LQG design. This adds to the complexity of the control design, limiting the bandwidth of the implementation. For the bandwidth of interest, from 30 to 900 Hz, the FIR filter order was limited to 48 by the digital processing necessary to implement the controller. The results of this design are illustrated in Figure 8. Comparison of this closed-loop response with the preceding results shows a similar behavior.

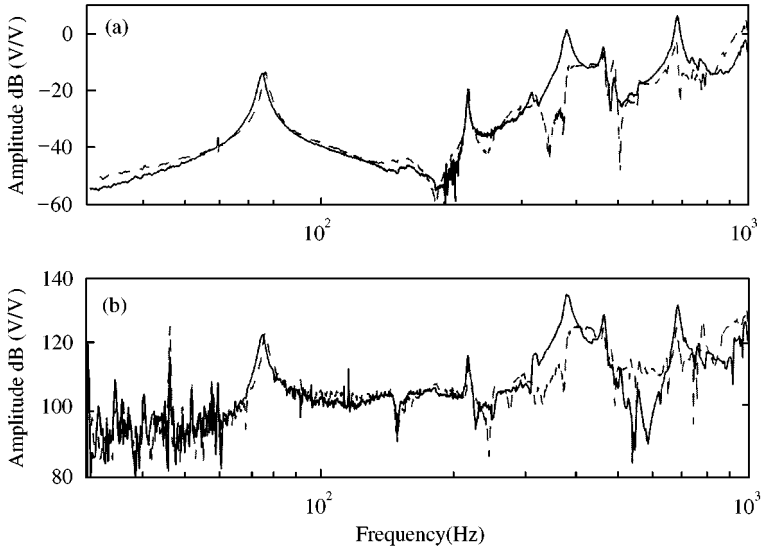

Figure 8. Performance of xLMS compensator, $n = 48$ (——, open loop; – – – –, closed loop). (a) Vibration performance 5·35 dB, (d) acoustic performance 3·07 dB.

The xLMS design does not attenuate the first resonant mode as heavily as the feedback designs, attaining the majority of the performance by reducing the response at higher frequencies. The overall performance of this design is slightly lower than that of other experiments reported in the literature. Jerome *et al.* [32] reported between 3 and 8 dB of radiated sound pressure reduction for a similar experiment using a single-input single-output controller with 50 coefficients. Clark *et al.* [33] reported between 5 and 10 dB of noise reduction when driving a plate far from one of its resonances, and showed that increasing the number of actuators and sensors results in increased performance. The authors attribute the lower performance obtained in this experiment to the broadband nature of the disturbance and to a smaller extent to the limited number of filter coefficients that could be implemented in real time.

5. SUMMARY OF RESULTS AND CONCLUSIONS

Achieving structural–acoustic control of complex engineering structures is known to be a challenging problem. This work demonstrates both the possibilities and limitations of using embedded actuation and structural sensing to reduce the radiated acoustic power by implementing a variety of control techniques on a representative composite panel structure. While this comparison is made on a simple representative structure, the conclusions are meant to be useful for more complex applications [20–23]. The results indicate that while significant broadband closed-loop performance can be achieved through a variety of compensation techniques, particular design methods and techniques offer superior performance based on the requirements and architecture of the individual system, as expected.

Two types of comparisons can be made between the compensator designs presented. First, each control design is based on a specific architecture possessing particular limitations that should be understood (Table 1). Depending on the configuration of the

TABLE 1

Comparison between control architectures

	Capabilities	Limitations
Rate feedback	Simple design—no model necessary Low-order compensator	Limited performance/bandwidth Achieved performance is based on sensor location
Optimal feedback (LQG)	Higher performance/bandwidth than classical designs Acoustic performance metric can be directly included in cost expression	Accurate model necessary for design High order, complex compensator requiring iteration and engineering judgement in design
Adaptive feedforward (*x*LMS)	Adaptively tracks plant dynamics Simple design—single convergence parameter	Requires measurement of disturbance signal Time-domain design; performance prediction is based on simulation rather than frequency responses Requires broadband model for implementation

TABLE 2

Performance summary of closed-loop structural–acoustic control designs

Compensator	Performance (dB)		Implementation Limitation
	Vibration	Radiation	
Rate of feedback	0·83	1·96	Bandwidth limited by modal density
Frequency-weighted LQG (FW-LQG)	4·56	5·93	Small stability margins at (3, 1) structural mode
Radiation filter LQG (RF-LQG)	4·27	4·13	Small stability margins at (3, 1) structural mode
*x*LMS feedforward	5·35	3·07	Adaptive filter size limited by digital hardware

structural–acoustic system, not all designs may be applicable. Second, the control designs can be compared based on performance since each compensator is implemented on a single test-bed under the same hardware constraint, and with a consistent method of measuring the performance (Table 2).

The results obtained in this research have, for the first time, experimentally verified the performance of an optimal controller based on acoustic radiation filters. Although the FW-LQG compensator achieved greater acoustic performance than the RF-LQG design, consideration of the sensor and actuator placement reveals that this result is dependent on the placement of the control sensor. The central location of the accelerometer sensor tends to make acoustically radiating modes particularly observable. Reducing this vibration sensor signal indirectly reduces the acoustic radiation. The performance of the FW-LQG design is also dependent on the particular tuning done heuristically by the control designer, while the RF-LQG controller directly reduces the acoustic radiation and is less sensitive to the placement of the structural sensor making it a more general solution for structural–acoustic control.

The results presented here have demonstrated the following advantages of LQG feedback control using the radiation filter acoustic model. First, optimal control techniques (LQG) in general achieve significant performance gains compared with simpler classical techniques. Second, although the xLMS adaptive feedforward compensator is capable of similar broadband performance, it requires a known disturbance and a structural model of the same order to be implemented with a reasonably size adaptive filter. The xLMS algorithm does have the advantage of being more robust to errors in the control-to-error model. Lastly, the radiation filter formulation, using the far field acoustic power explicitly in the optimal cost function, being therefore less sensitive to the sensor/actuator architecture, is a more general approach to the problem of adaptive structural–acoustic control.

ACKNOWLEDGMENTS

The authors would like to acknowledge the support of the Army Research Office Multidisciplinary University Research Initiative, under Grant DAAH04-95-1-0104, and Dr Gary Anderson, the technical monitor.

REFERENCES

1. P. A. Nelson and S. J. Elliot 1992 *Active Control of Sound*. New York: Academic Press.
2. P. A. Nelson, A. R. D. Curtis and S. J. Elliot 1986 *Journal of Sound and Vibration* **105**, 173–178. The minimum power output of a pair of free field monopoles.
3. S. J. Elliot, I. M. Stothers and P. A. Nelson 1987 *IEEE Transactions on Acoustics, Speech and Signal Processing* **35**, 1423–1434. A multiple error LMS algorithm and its application to the active control of sound and vibration.
4. C. R. Fuller, C. H. Hansen and S. D. Snyder 1991 *Journal of Sound and Vibration* **145**, 195–215. Active control of sound radiation from a vibrating rectangular panel by sound sources and vibration inputs: an experimental comparison.
5. C. R. Fuller, C. A. Rogers and H. H. Robertshaw 1992 *Journal of Sound and Vibration* **157**, 19–39. Control of sound radiation with active/adaptive structures.
6. J. P. Maillard and C. R. Fuller 1999 *Journal of Sound and Vibration* **222**, 363–388. Active control of sound radiation from cylinders with piezoelectric actuators and structural–acoustic sensing.
7. R. A. Burdisso, J. S. Vipperman and C. R. Fuller 1993 *Journal of the Acoustical Society of America* **94**, 234–242. Causality analysis of feedforward-controlled systems with broadband input.
8. R. L. Clark and C. R. Fuller 1991 *Journal of Intelligent Materials Systems and Structures* **2**, 431–452. Control of sound radiation with adaptive structures.
9. J. S. Vipperman, R. A. Burdisso and C. R. Fuller 1993 *Journal of Sound and Vibration* **166**, 283–299. Active control of broadband structural vibration using the LMS adaptive algorithm.
10. M. Fripp, D. Q. O'Sullivan, S. R. Hall, N. W. Hagood and K. Lilienkamp 1997 *Proceedings of the SPIE* **3041**, 88–99. Test-bed design and modelling for aircraft interior acoustic control.
11. B. S. Bingham and N. W. Hagood 1998 *AMSL Report* 98-5, *Massachusetts Institute of Technology*. Structural–acoustic design and control of an integrally actuated composite panel.
12. R. R. Craig, Jr 1981 *Structural Dynamics: An Introduction to Computer Models*. New York: John Wiley and Sons.
13. R. M. Jones 1975 *Mechanics of Composite Materials*. Washington, DC: Hemisphere Publishing Corporation.
14. W. T. Baumann, F. Ho and H. H. Robertshaw 1994 *Journal of the Acoustical Society of America* **92,** 1998–2011. Active structural acoustic control of broadband disturbances.
15. C. E. Wallace 1972 *The Journal of the Acoustical Society of America* **51**, 946–952. Radiation resistance of a rectangular panel.
16. F. Francis 1987 *An Introductory Course in H^∞ Control*, Berlin: Springer-Verlag.
17. P. VanOverschee, B. DeMoor, W. Dehandschutter and J. Swevers 1997 *Automatica* **33**, 2147–2157. A sub-space algorithm for identification of discrete time frequency domain power spectra.

18. W. DEHANDSCHUTTER, K. HENRIOULLE, J. SWEVERS and P. SAS 1997 *EAA International Symposium on Active Control of Sound and Vibration-ACTIVE 97*, 979–993. State space feedback control of sound radiation using structural sensors and structural control inputs.
19. J. P. ROGERS and N. W. HAGOOD 1998 *Proceedings of the Nineth International Conference on Adaptive Structures and Technologies-ICAST*, 203–212. Hover testing of a 1/6th Mach scale CH-47D blade with integral twist actuation.
20. C. A. SAVRAN, M. J. ATALLA and S. R. HALL 2000 *Proceedings of the SPIE Conference on Mathematics and Control in Smart Structures*, 137–147. Broadband active structural–acoustic control of a fuselage test-bed using collocated piezoelectric sensors and actuators.
21. M. L. FRIPP, M. J. ATALLA, N. W. HAGOOD, C. SAVRAN and S. TISTAERT 1999 *Proceedings of the 10th International Conference on Adaptive Structures and Technologies-ICAST*, 447–456. Reconfigurable arrays for broadband feedback control of aircraft fuselage vibrations.
22. M. L. R. FRIPP, M. J. ATALLA and N. W. HAGOOD 2000 *Proceedings of the SPIE Conference on Mathematics and Control in Smart Structures*, 540–552. Reconfigurable arrays of collocated sensors and actuators for modal isolation.
23. K. SONG, M. J. ATALLA and S. R. HALL 2000 *Proceedings of the SPIE Conference on Mathematics and Control in Smart Structures*, 112–124. Active structural-acoustic control of a think-walled cylindrical shell.
24. A. BENT and N. HAGOOD 1997 *Journal of Intelligent Material Systems and Structures* **8,** 903–919. Piezoelectric fiber composites with interdigitated electrodes.
25. M. E. CAMPBELL 1993 *M.S. Thesis, Massachusetts Institute of Technology*. Neo-classical control of structures.
26. K. ZHOU, J. C. DOYLE and K. GLOVER 1995 *Robust and Optimal Control*. Englewood Cliffs, NJ: Prentice-Hall.
27. W. S. LEVINE 1993 *The Control Handbook*. Boca Raton, FL: CRC Press Inc.
28. R. N. JACQUES 1994 *Ph.D. Thesis, Massachusetts Institute of Technology*. On-line system identification and control design for flexible structures.
29. S. HAYKIN 1994 *Introduction to Adaptive Filters*. New York: MacMillan Publishing Company.
30. S. J. ELLIOT, I. M. STOTHERS and P. A. NELSON 1987 *IEEE Transactions on Acoustics, Speech, and Signal Processing* **35**, 1423–1435. A multiple error lms algorithm and its application to the active control of sound and vibration.
31. J. S. VIPPERMAN, R. A. BURTDISSO and C. R. FULLER 1993 *Journal of Sound and Vibration* **166**, 283–299. Active control of broadband structural vibration using the LMS adaptive algorithm.
32. J. P. SMITH, C. R. FULLER and R. A. BURDISSO 1996 *Journal of Intelligent Material Systems and Structures* **7**, 54–64. Control of broadband acoustic radiation with adaptive structures.
33. R. L. CLARK and C. R. FULLER 1992 *Journal of the Acoustical Society of America* **91**, 3313–3320. Experiments on active control of structurally radiated sound using multiple piezoceramic actuators.